

NUMERICAL INVESTIGATION OF THE FLOW FEATURES ON THE TURRET WITH DIFFERENT CYLINDER HEIGHT IN THE TRANSONIC FLOW

Xiao-Tong Tan^{1,2}, He-Yong Xu^{1,2}, Zhen Pei^{1,2}

¹School of Aeronautics, Northwestern Polytechnical University, Xi'an 710072, China; ²National Key Laboratory of Aircraft Configuration Design, Xi'an 710072, China

Abstract

Improved delayed detached eddy simulation is performed to investigate the transonic flow around the turret at Ma=0.7 and Re=9.15×105. Five cases correspond to different cylinder heights for the turret, whose heights are 0, 0.25R, 0.5R, 0.75R and R, respectively. Proper orthogonal decomposition and dynamic mode decomposition are used to analyze the flow field data. There are basic features around the turret, including necklace vortices, shock wave, shear layer, turbulent wakes and shock/boundary-layer interaction. Two unsteady shock-wake-correlated modes, the asymmetric shifting mode and the symmetric breathing mode, are observed in flow analysis. With the increasing of the cylinder height, both the relative energy of shock and the range of shock jitter gradually increase. The relative energy increases from 26% to 59%, and the range of shock jitter goes from 16° to 34°. The POD analysis yields the single peak frequency for two dominant modes. The peak frequencies of the "shifting" mode are generally at StD < 0.23, while the peak frequencies of the "breathing" mode are generally at StD > 0.26. The DMD analysis gives the range of the peak frequencies of the "breathing" mode are StD = 0.26-0.41. It can be concluded that the frequency of the shedding vortex and shock motion are not sensitive to the cylinder height.

Keywords: improved delayed detached eddy simulation, shock jitter, proper orthogonal decomposition, dynamic mode decomposition

1. Introduction

Aero-optical effect refers that the beam passing through the nonuniform flow field, causes the beam defocus, pointing errors, and violent energy reduction^{[1][2][3]}. Due to the advent of laser weapons on the airplane in the 1960s, the aero-optical effect is paid much attention. Many aero-optical system configurations chose the hemisphere-on-cylinder turret^[4]. However, extending a protuberance into the high-speed flow is often accompanied by adverse aerodynamic issues such as the necklace vortices and massively separated flow. When the inflow is at transonic speed, the shockwave occurs on the turret dome^[5]. These flow structures negatively affect the performance of the beam transmission, as well as create structural issues from the cyclic loading caused by the unsteady flow^[1].

In the context of the transonic flow, the incoming flow is usually greater than Ma=0.55, and locally supersonic region appears on the turret dome. Since then, several researchers have investigated the transonic turret flow through the computational studies^{[5]-[8]}, wind-tunnel testing^[9], and flight-testing^[10]. Malkus et. al^[5] investigated the effects of varying submergence on the transonic flow past canonical wall-mounted hemispheres at a freestream Mach number Ma=0.8. Proper orthogonal decomposition^[13] (POD) and dynamic mode decomposition^[14] (DMD) were used to analyze the flow field data, and two wake modes were identified, designated a "shifting" mode and a "breathing" mode. The "shifting" mode arises from the correlation between vortices shedding off alternating sides of the hemisphere and large spanwise shifting of the wake, while the "breathing" mode is associated with the correlation between the spanwise symmetric shedding and the breathing type motion of the wake. More POD and DMD analysis on the flow field data for the turret can be found in Refs. [11] and [12]. While the current studies for the turret are hemisphere model^{[11][12][14]} and hemisphere-on-cylinder

NUMERICAL INVESTIGATION OF THE FLOW FEATURES ON THE TURRET WITH DIFFERENT CYLINDER HEIGHT IN THE TRANSONIC FLOW

model^[15], there is a current lack of the investigation on height of cylinder affecting flow structures and beam transmission. In the present study, improved delayed detached eddy simulation^[16] (IDDES) is performed to investigate the effect of varying heights of cylinder on the turret at the transonic Mach number Ma=0.7. Five levels of height are discussed, ranging from 0 to R, where R is the hemispherical radius. Instantaneous and mean flow field results are discussed, including the flow features and the location of the shock. In addition, POD and DMD are performed on flow data to further investigate the spatial and temporal characteristics of the dominant unsteady modes. Finally, time-averaged optical results are conducted to quantify the effect of the different height of cylinder for the turret.

2. Simulation Method

The fluid dynamics and optical transmission are decoupled to simulate the aero-optical effect of the turret. The five cases correspond to different cylinder heights for the turret, whose heights are 0, 0.25R, 0.5R, 0.75R and R, respectively, shown in Figure 1. The radius of the hemisphere is R = 70mm. The Reynolds number based on the radius of the sphere is $R = 9.15 \times 10^5$ and the Mach number is M = 0.7.

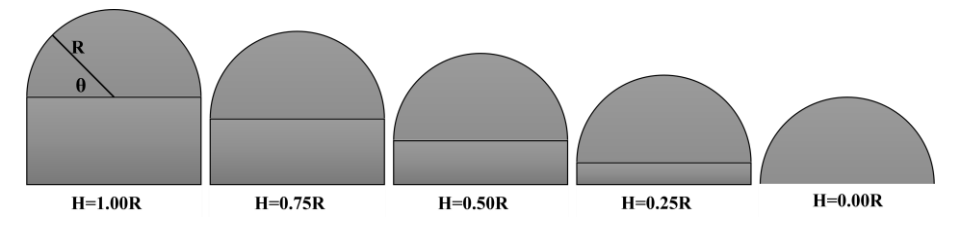


Figure 1 – Schematic of varying heights of cylinder on the turret.

The stable freestream flow would form a complex wake behind the turret, a computational domain consisting of a quarter sphere and a half-cylinder, shown in Figure 2. To avoid the influence of far-field boundaries, the radius of the quarter sphere is 40R, and the length of the half cylinder is 80R. The height of the first layer of the grid is 4×10^{-5} R, thus ensuring $y^+ < 1$. The total grid number of five cases is about 17 million, respectively.

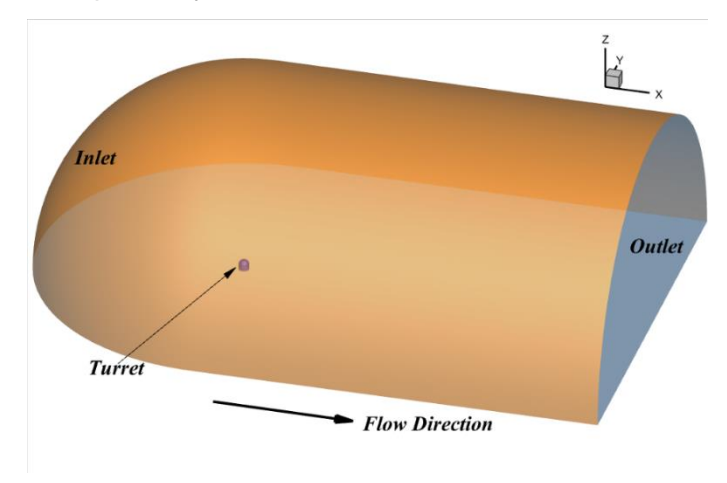


Figure 2 – Computational domain for simulation.

To capture turbulent structures in the flow field, the IDDES turbulent model is applied to perform transient simulation. As an extension of DES, IDDES allows RANS to be a much thinner near-wall region, where the wall distance is much smaller than the boundary layer thickness. The IDDES was proposed aiming at extending the DDES with the capability of the WMLES. The IDDES hybridizes the applications both for the DDES and MWLES uses with a single set of formulas. The formulations of the DDES and WMLES are presented in the work by Shur et al. [17], therefore, only hybridization of DDES and WMLES is introduced below. For the IDDES, the specific dissipation rate ω in the SSTKO model can be replaced by $\widetilde{\omega}$ (hereafter referred to as IDDES-SSTKO).

$$\omega = \frac{\sqrt{k}}{l_{HYBRID}\beta^* f_{\beta^*}} \tag{1}$$

Where $\beta = 0.09$, and

NUMERICAL INVESTIGATION OF THE FLOW FEATURES ON THE TURRET WITH DIFFERENT CYLINDER HEIGHT IN THE TRANSONIC FLOW

$$\begin{cases} f_{\beta^*} = \begin{cases} 1 & \text{for } \chi_k \le 0\\ \frac{1 + 680\chi_k^2}{1 + 400\chi_k^2} & \text{for } \chi_k \le 0 \end{cases} \\ \chi_k = \frac{\nabla k \cdot \nabla \omega}{\omega^3} \end{cases}$$

$$l_{HYBRD} = f_d \left(1 + f_e \right) l_t + \left(1 - f_d \right) C_{DES} \Delta_{DDES}$$
(2)

The blending function \widetilde{f}_d is defined by

$$f_d = \max\left(\left(1 - f_{dt}\right), f_B\right) \tag{3}$$

With

$$f_{dt} = 1 - \tanh \left[\left(C_{dt} \frac{v_t}{\sqrt{\nabla v : \nabla v^T \kappa^2 d^2}} \right) \right]$$
(4)

Where κ is the von Karman constant.

As for f_R , it is defined as

$$f_B = \min\left[2\exp\left(-9\left(0.25 - \frac{d^2}{\Delta}\right)\right), 1\right]$$
 (5)

Where Δ is needed sub-grid length-scale, and d is the distance to the wall.

3. Results

3.1 Flow field results

Several basic flow features are showed in Figure 3, contoured by the density gradient. Upstream of the turret, a turbulent boundary layer develops on the plate and a circulating large-scale vortical structure is formed. The transonic shock above the turret is also visible. When the flow passes through the shock, a separated shear layer appears. Further, the separated shear layer occurs the Kelvin–Helmholtz (K-H) instability, causing the abundant turbulent wakes.

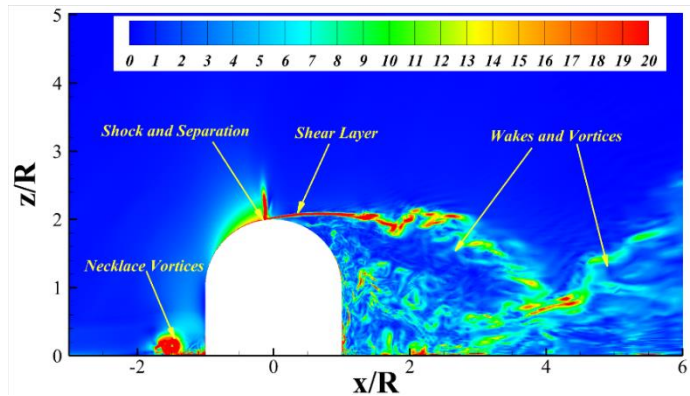


Figure 3 - The instantaneous flow structures in centerline plane, contoured by the density gradient. Figure 4 displays the mean pressure coefficient on the centerline of the turret. For the case of H=1R, the simulation result is consistent with the experimental data^[18]. It can be seen that as the cylinder height increases, the mean pressure coefficient decreases, and the position of the pressure minimum is gradually moving forward, ranging from 83° to 78°. For H=0R, H=0.25R and H=0.5R, the pressure distribution in front of the turret is affected by the necklace vortices. Especially the H=0R, the range of influence is up to 30 elevation angle.

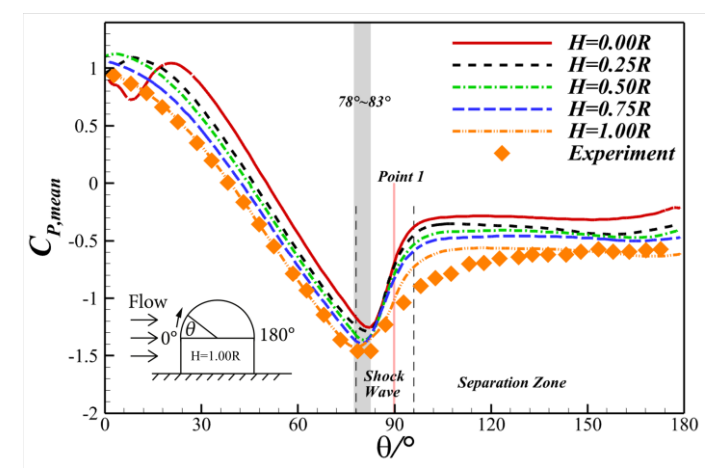


Figure 4 - Mean pressure coefficient on the centerline of the turret for varying heights.

The most important flow feature is the shock motion on the turret dome. The shock position is tracked using 500 instantaneous flow fields. Figure 4 shows the probability density functions (PDF) for the unsteady shock position for varying heights. Each shock position is measured at the height above the hemisphere surface r/H=1.1. The mean positions of the shock wave for five heights are at 88.32°, 88.17°, 88.04°, 87.57° and 87.17°, respectively. The mean range of the shockwave for five heights are approximately 16°, 20°, 22°, 26° and 34°, respectively.

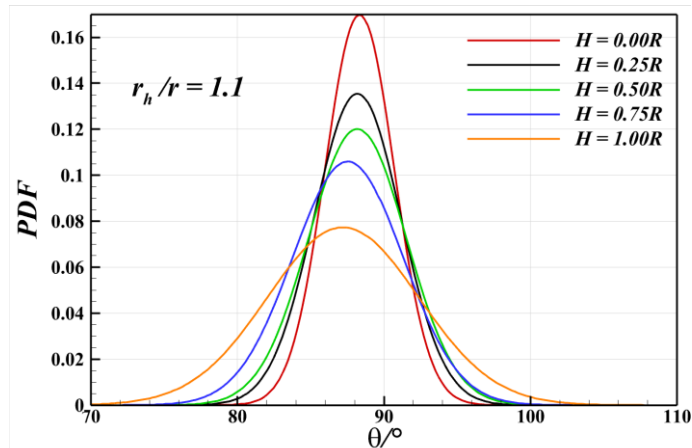


Figure 5 - The PDF of shockwave location.

3.2 POD Analysis

Modal analysis can yield substantial insights into turbulent flow^[19]. The correlation between the unsteady transonic shock and the shedding vortex is further investigated using POD. Here, 500 snapshots are collected every 5 timesteps. The POD modal energy is presented in two ways in Figure 6. The left plot is the cumulative POD energy. It can be seen that the energy of the first 30 modes accounts for 90%. The case of H=1R has the largest relative energy in the first 30 modes. Except the case of H=1R, the case of H=0.5R has relatively large energy. The cases of H=0.25R and H=0.75R have the similar relative energy in the first 30 modes. The conclusion is also obtained in the right plot. In addition, only the first two modes have the relative energy, which are bigger than 10%. Therefore, the first two modes are further investigated.

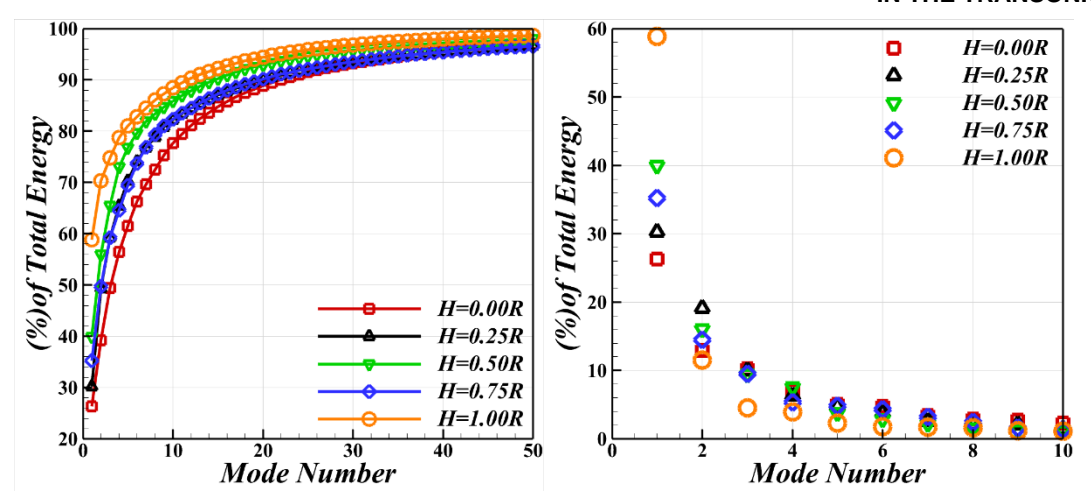


Figure 6 - Cumulative energy in POD mode and POD energy distribution per mode.

The first POD mode, which represents the most dominant flow structure in each case, is showed in Figure 7. For the cases of H=0R, 0.75R and H=1R, the first POD modes display the "breathing" mode. The behavior of this mode represents the streamwise shock motion across the dome of the turret with large spanwise shedding of symmetric wake structures. For the cases of H=0.25R and H=0.5R, the first POD mode displays the "shifting" mode, representing shock motion and spanwise asymmetric wake shedding. In addition, with the increasing of height, the first mode accounts for more relative energy, which illustrates the unsteady shock on the dome of turret play a leading role in the flow field.

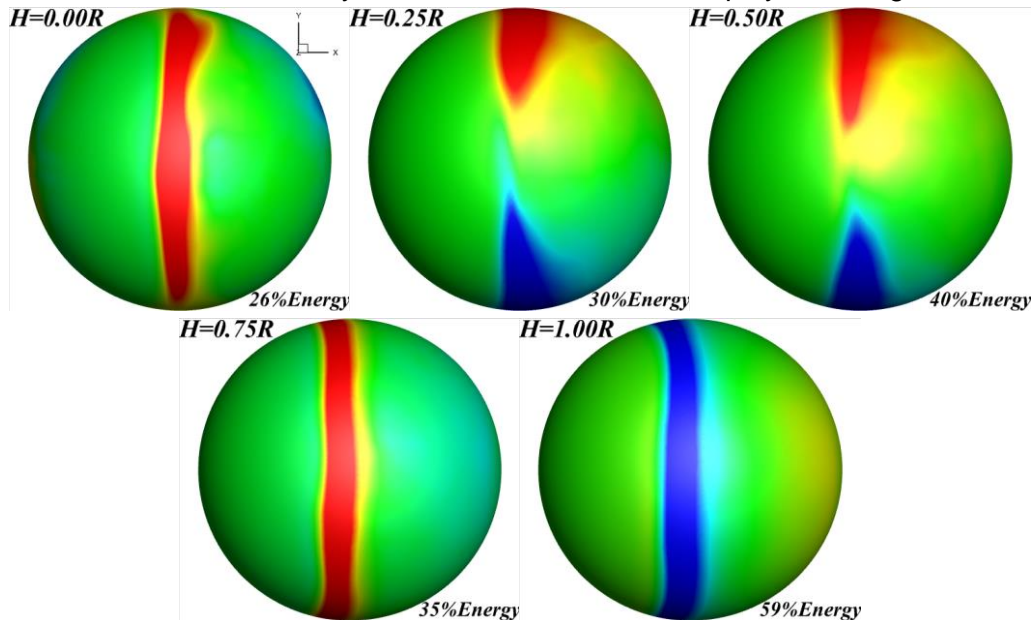
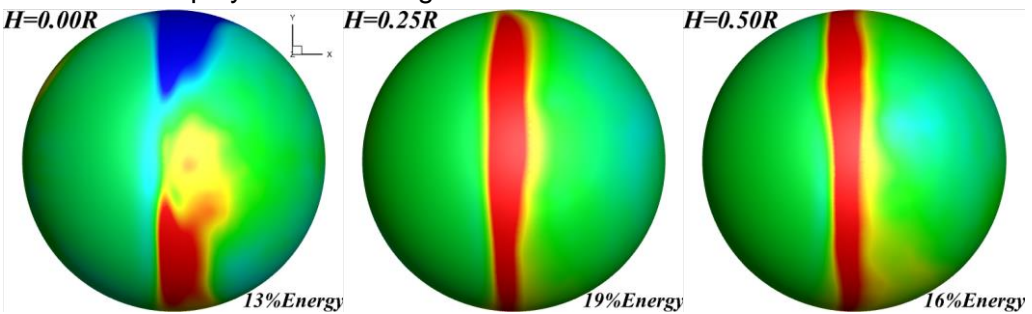


Figure 7 - The first mode for five heights in POD analysis.

The second POD mode, which represents the second most dominant structure in each case, is shown in Figure 8. The cases of H=0R, 0.75R and H=1R display the "shifting" mode, and the cases of H=0.25R and H=0.5R display the "breathing" mode.



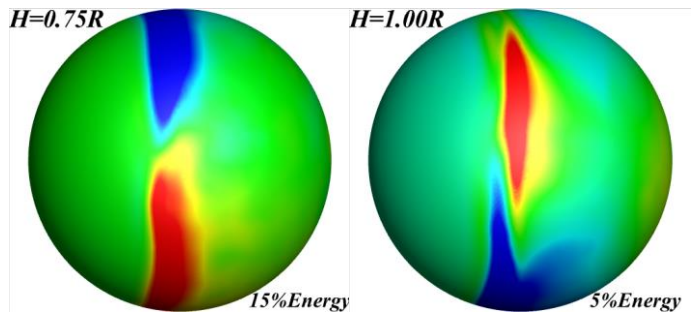
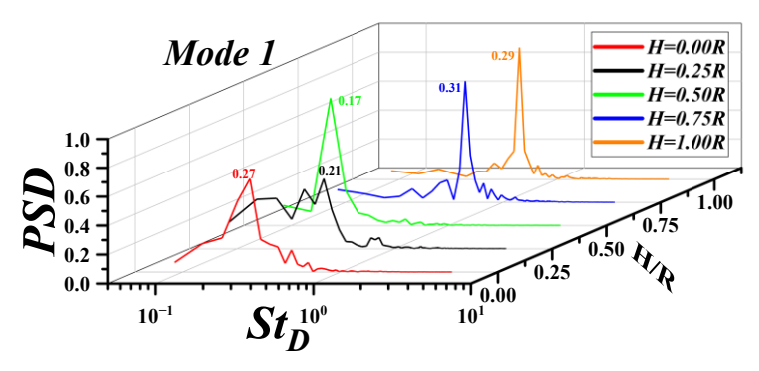
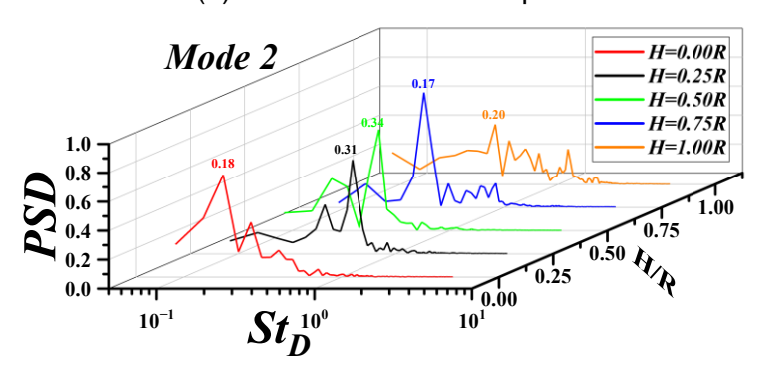


Figure 8 - The second mode for five heights in POD analysis.

The fast Fourier transform (FFT) plots of the temporal coefficient for the dominant POD modes for varying heights are shown in Figure 9. The peak frequencies of the first mode for H=0.25R and H=0.5R are in the range of St_D = 0.17-0.21. The peak frequencies of first mode for the others are in the range of St_D = 0.27-0.31. Similarly, the peak frequencies of the second mode for H=0.25R and H=0.5R are in the range of St_D = 0.31-0.34. The peak frequencies of the second mode for the others are in the range of St_D = 0.17-0.20.







(b) The second POD mode spectra

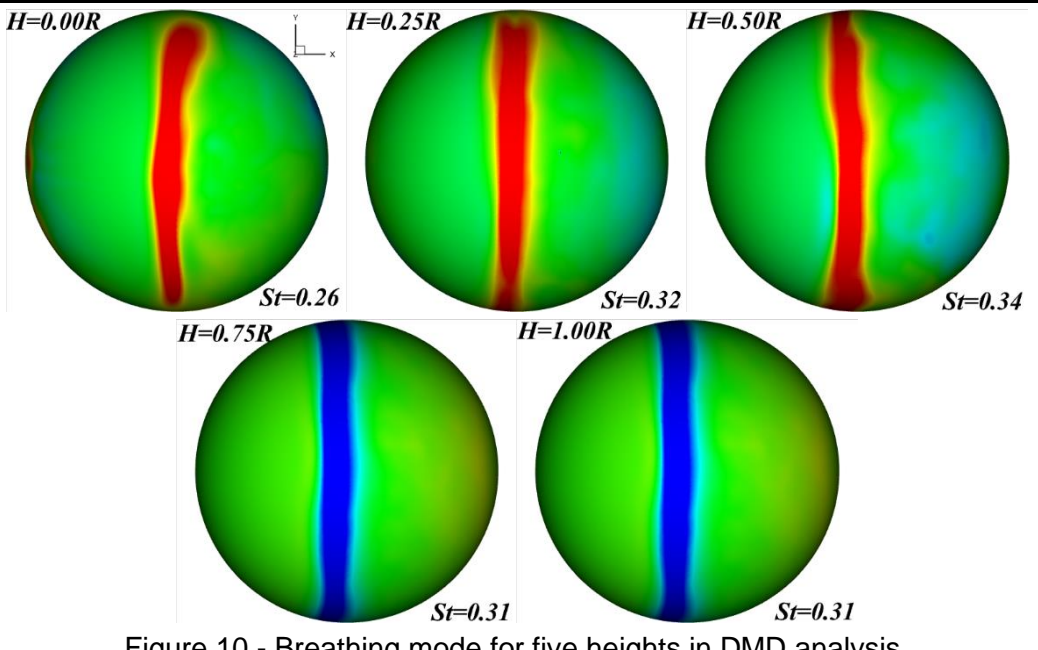
Figure 9 - Spectral content for POD temporal coefficients for five heights.

3.3 DMD Analysis

To further analyze the frequencies of these modes, DMD is used as a companion analysis tool to POD. Table 1 displays the peak frequencies of dominant modes for varying heights using POD and DMD analysis. It is obvious that the peak frequencies of the "shifting" mode are generally less than that of the "breathing" mode. The peak frequencies of the "shifting" mode are generally at $St_D > 0.26$. Moreover, the POD analysis only displays the single peak frequency, but DMD analysis can give the range of the peak frequency. Figure 10 and Figure 11 are the "breathing" mode and "shifting" mode in DMD analysis, respectively. DMD also have the ability to obtain the "shifting" mode and "breathing" mode. For five heights, the frequency of the "breathing" is about two times than that of the "shifting" mode. It is concluded that the frequency of the shedding vortex and shock motion are no sensitive to the cylinder height.

Table 1 - The peak frequencies of dominant modes for varying heights using the POD and DMD analysis.

	POD		DMD	
	Breathing	Shifting	Breathing	Shifting
H=0.00R	0.27	0.18	0.26~0.40	0.13~0.21
H=0.25R	0.31	0.21	0.27~0.41	0.13~0.23
H=0.50R	0.34	0.17	0.27~0.41	0.11~0.23
H=0.75R	0.31	0.17	0.26~0.41	0.11~0.22
H=1.00R	0.29	0.20	0.26~0.41	0.11~0.22



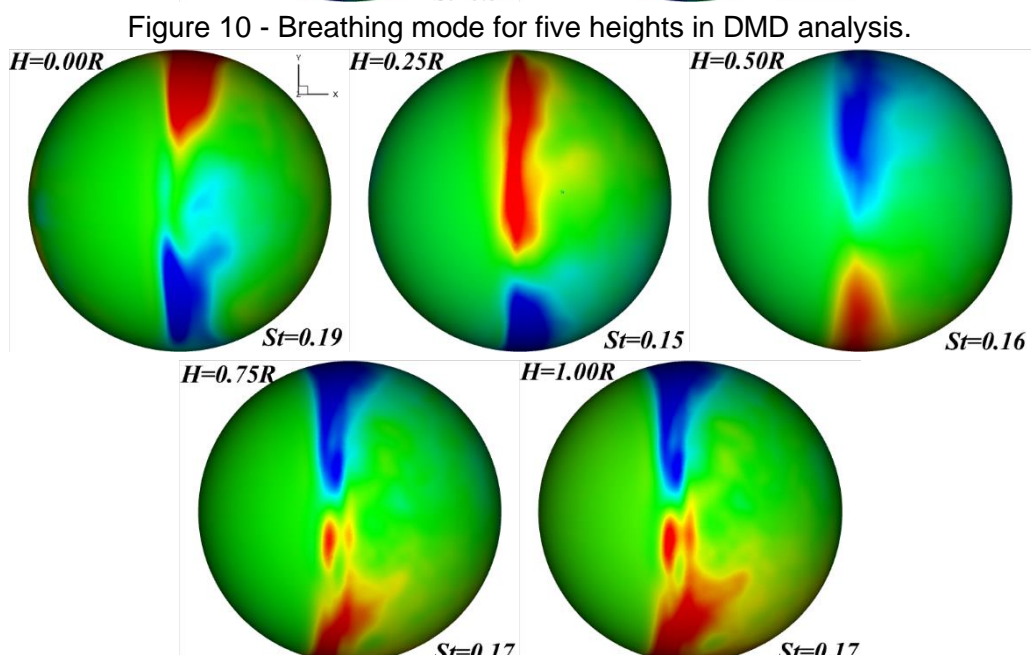


Figure 11 - Shifting mode for five heights in DMD analysis.

4. Conclusions

In this work, the flow around the turret at Ma=0.7 is investigated using IDDES to compare the flow features for five cylinder heights. The cylinder heights range from 0R to 1R. POD and DMD are also applied to analyze the effect of cylinder height.

For five heights, there are basic features around the turret in transonic flow, including necklace vortices, shock wave, shear layer, turbulent wakes and shock/boundary-layer interaction. Two unsteady shock-wake-correlated modes, the asymmetric shifting mode and the symmetric breathing mode, are observed in flow analysis. However, with the increasing of the cylinder height, both the

NUMERICAL INVESTIGATION OF THE FLOW FEATURES ON THE TURRET WITH DIFFERENT CYLINDER HEIGHT IN THE TRANSONIC FLOW

relative energy of shock and the range of shock jitter gradually increase. The relative energy increases from 26% to 59%, and the range of shock jitter goes from 16° to 34°.

The POD analysis yields the single peak frequency for two dominant modes. The peak frequencies of the "shifting" mode are generally at $St_D < 0.23$, while the peak frequencies of the "breathing" mode are generally at $St_D > 0.26$. The DMD analysis give the range of the peak frequency. For five heights, the peak frequencies of the "shifting" mode are $St_D = 0.11$ -0.23, and the peak frequencies of the "breathing" mode are $St_D = 0.26$ -0.41. It can be concluded that the frequency of the shedding vortex and shock motion are no sensitive to the cylinder height.

5. Acknowledgements

The author(s) disclosed receipt of the following financial support for the research, authorship, and/or publication of this article: The work is funded by the National Key Lab Foundation with Grant No. 2020KLF030101.

6. Contact Author Email Address

Electronic mail: 2020260145@mail.nwpu.edu.cn

Electronic mail: xuheyong@nwpu.edu.cn

7. Copyright Statement

The authors confirm that they, and/or their company or organization, hold copyright on all of the original material included in this paper. The authors also confirm that they have obtained permission, from the copyright holder of any third party material included in this paper, to publish it as part of their paper. The authors confirm that they give permission, or have obtained permission from the copyright holder of this paper, for the publication and distribution of this paper as part of the ICAS proceedings or as individual off-prints from the proceedings.

References

- [1] Mcalister K, Pucci S, Mccroskey W, et al. An experimental study of dynamic stall on advanced airfoil sections. *NASA Technical Memorandum 84245*, Vol. 2, pressure and force data, 1982. S. Gordeyev and E. Jumper, Fluid dynamics and aero-optics of turrets. *Prog. Aerosp. Sci*, Vol. 46, pp 388-400, 2010.
- [2] Wang M, Mani A, and Gordeyev S, Physics and computation of aero-optics. *Annu. Rev. Fluid Mech*, Vol. 44, pp 299-321, 2012.
- [3] Jumper E. J, Gordeyev S, Physics and measurement of aero-optical effects: past and present. *Annu. Rev. Fluid. Mech.*, Vol. 49, pp 419-441, 2017.
- [4] Gordeyev S, Cress J A, Smith A, and Jumper E J, Aero-optical measurements in a subsonic, turbulent boundary layer with non-adiabatic walls. *Phys. Fluids*, Vol. 27, 045110, 2015.
- [5] Malkus M J, Frede M T, Sherer S E and Garmann D J, Effect of submergence on transonic flow around a hemisphere. *AlAA J.*, Vol. 60, No. 11, pp 6082-6096, 2022.
- [6] Jelic R, Sherer S E, and Greendyke R, Simulations of various turrets and subsonic and transonic flight conditions using OVERFLOW. *J. Aircr.*, Vol. 50, No. 2, pp 398-409, 2013.
- [7] Coirer W J, Porter C, Barber J, and Stutts J, Aero-optical evaluation of notional turrets in subsonic, transonic and supersonic regimes. *AIAA Paper*, No.2014-2355, 2014.
- [8] Weston D B, Sherer S E, Comparison of computational and experimental results on a transonic hemisphere. *AIAA Paper*, No.2019-1901, 2019.
- [9] Beresh S J, Henfling J F, Spillers R W, and Pruett B M, Unsteady shock motion in a transonic flow over a wall-mounted hemisphere. *AIAA J.*, Vol. 54, No. 11, pp 3509-3515, 2016.
- [10]Jumper E, Gordeyev S, Cavalieri D, and Rollins P, Airborne aero-optics laboratory transonic (AAOL-T). *AIAA Paper*, No.2015-0675, 2015.
- [11]Abado S, Gordeyev S, and Jumper E, Approach for two-dimensional velocity mapping. *Optical Engineering*, Vol. 52, No. 7, 071402, 2013.
- [12]De L N, Gordeyev S, Jumper E, In-flight aero-optics of the turrets. *Optical Engineering*, Vol. 52, No. 7, 071405, 2013.
- [13]Taira K, Brunton S L, Dawson S T and Rowley C W, Modal analysis of fluid flows: an overview. *AIAA J.*, Vol. 55, No. 12, pp 4013-4041, 2017.
- [14]Schmid P J, Dynamic mode decomposition of numerical and experimental data. *J. Fluid Mech*, Vol. 656, pp 5-28, 2010.
- [15]Ren X, Yu H H, Yao X H, Su H and Hu P, Passive fluidic control on aero-optics of transonic flow over turrets with rough walls. *Phys. Fluids*, Vol. 34, 115109, 2022.

NUMERICAL INVESTIGATION OF THE FLOW FEATURES ON THE TURRET WITH DIFFERENT CYLINDER HEIGHT IN THE TRANSONIC FLOW

- [16]Yin Z, Reddy K R, and Durbin P A, On the dynamic computation of the model constant in delayed detached eddy simulation. *Phys. Fluids*, Vol. 27, 025105, 2015.
- [17]Shur M L, Spalart P R, Strelets M K, and Travin A K, A hybrid RANS-LES approach with delayed-DES and wall-modelled les capabilities. *Int. J. Heat Fluid Flow*, Vol. 29, pp 1638-1649, 2008.
- [18]Ren X, Yu H H, Yao X H, Su H, and Hu P, Shock boundary layer interaction and aero-optical effects in a transonic flow over hemisphere-on-cylinder turrets. *Int. J. Aerosp. Eng.*, 397763, 2022.
- [19]Taira K, Brunton S L, Dawson S T, Modal analysis of fluid flows: an overview. *AIAA J.*, Vol. 55, No. 12, pp 4013-4041, 2017.